

LHC Data and Aspects of New Physics

Tommi Alanne ^{a,b*}, Stefano Di Chiara^{a†}, and Kimmo Tuominen ^{a,b‡}

^a *Helsinki Institute of Physics, P.O.Box 64, FI-000140, Univ. of Helsinki, Finland and*

^b *Department of Physics, P.O.Box 35, FI-40014, Univ. of Jyväskylä, Finland*

Abstract

We consider the implications of current LHC data on new physics with strongly interacting sector(s). We parametrize the relevant interaction Lagrangian and study the best fit values in light of current data. These are then considered within a simple framework of bosonic technicolor. We consider first the effective Lagrangian containing only spin-0 composites of the underlying theory, which corresponds to a two Higgs doublet model. With respect to this baseline, the effects of the vector bosons, a staple in strong interacting theories, are illustrated by considering two cases: first, the case where the effects of the vector bosons arise only through their mixing with the electroweak $SU(2)_L$ gauge fields and, second, the case where also a direct interaction term with neutral scalars exists. We find that the case of a W' coupling to the Higgs boson only via the mixing of vector fields produces a negligible improvement in the fit of the present data, while even a small direct coupling of the composite vector fields to the Higgs allows the tested model to fit optimally the experimental results.

* tommi.alanne@jyu.fi

† stefano.dichiara@helsinki.fi

‡ kimmo.i.tuominen@jyu.fi

I. INTRODUCTION

The recent discovery of a light scalar with properties compatible with those of the Standard Model (SM) Higgs boson, h^0 , imposes new experimental tests on previously viable beyond the Standard Model (BSM) theory frameworks. Fervent activity in this direction has focused mostly on the possibility that a new charged particle could enhance the Higgs decay rate to two photons [1–13]. This is measured at LHC and Tevatron, with the full dataset, to be slightly enhanced compared to the SM prediction [14–16], with the diphoton signal strength equal to 1.65 ± 0.32 at ATLAS and 1.11 ± 0.31 at CMS.¹ While most of the efforts were focused on the Higgs physics associated with a new charged scalar or a vector fermion, both of which naturally arise in supersymmetry [17–23] or composite Higgs frameworks [24–27], less extensive research has been conducted recently on the possibility that a heavy charged vector boson be responsible for the observed deviations of the Higgs couplings from the corresponding SM predictions [9, 28–30].

A heavy charged vector boson is naturally predicted by phenomenological theories featuring additional gauge groups, like Technicolor, Little Higgs, and Kaluza-Klein models [31–36]. In this paper we want to explore the effect of couplings of a heavy W' boson to the Higgs on LHC and Tevatron observables. To approach this task we first, in Section II, perform a fit with the parameters of a simple effective Lagrangian featuring rescaled Higgs couplings to SM particles as well as to a heavy charged scalar and a heavy charged vector boson. To have a concrete model to test against the results of the general fit, in Section III we introduce a low energy effective Lagrangian for a simple bosonic technicolor model, the bosonic Next to Minimal Walking Technicolor (bNMWT) [37–40]. The low energy effective Lagrangian for the scalar sector of bNMWT corresponds to a Type-I Two Higgs Doublet Model (2HDM) [41]. We scan the allowed parameter space of this model for data points viable under direct search constraints and electroweak (EW) precision tests, compare the data points to the measured Higgs physics observables, and find the optimal fit of the model. In Section IV we introduce two composite vector boson triplets in the low energy Lagrangian, while conserving gauge invariance at the microscopic level, which both mix with the SM W^\pm and directly couple to h^0 , and repeat the goodness of fit analysis above to determine the optimal values

¹ We use the more traditional "cut based" CMS result for the Higgs decay to diphoton.

of the W' and W'' couplings to h^0 . We illustrate separately the features which originate from the mixing and from the direct coupling. Our essential conclusion is that mixing alone produces a negligible improvement of the fit to the current data. A direct interaction on the other hand makes the bNMWT model a perfectly viable candidate.

II. LHC AND TEVATRON DATA FIT

The experimental results are expressed in terms of the signal strengths, defined as

$$\hat{\mu}_{ij} = \frac{\sigma_{\text{tot}} \text{Br}_{ij}}{\sigma_{\text{tot}}^{\text{SM}} \text{Br}_{ij}^{\text{SM}}} , \quad \sigma_{\text{tot}} = \sum_{\Omega=h, q\bar{q}, \dots} \epsilon_{\Omega} \sigma_{\omega \rightarrow \Omega} , \quad \omega = pp, p\bar{p} , \quad (1)$$

where ϵ_{Ω} is the efficiency associated with the given final state Ω in an exclusive search, while for inclusive searches one simply has $\sigma_{\text{tot}} = \sigma_{pp \rightarrow h(X)}$, the h production total cross section. The signal strengths from ATLAS, CMS, and Tevatron are given in Table I. All results for

ij	ATLAS	CMS	Tevatron
ZZ	1.50 ± 0.40	0.91 ± 0.27	
$\gamma\gamma$	1.65 ± 0.32	1.11 ± 0.31	6.20 ± 3.30
WW	1.01 ± 0.31	0.76 ± 0.21	0.89 ± 0.89
$\tau\tau$	0.70 ± 0.70	1.10 ± 0.40	
$b\bar{b}$	-0.40 ± 1.10	1.30 ± 0.70	1.54 ± 0.77

TABLE I: Data on inclusive channels from LHC and Tevatron experiments.

Higgs decays to bosons at ATLAS [14, 42, 43] and CMS [15, 44, 45], as well as the decay to $\tau\tau$ at CMS [46] and the Tevatron results [16], use the full respective dataset, while results for the decay to $b\bar{b}$ at ATLAS [47] and CMS [48], and to $\tau\tau$ at ATLAS [49], use $12 - 13 \text{ fb}^{-1}$ of integrated luminosity at 8 TeV and 5 fb^{-1} at 7 TeV. The $b\bar{b}$ quark pair is produced in association with a vector boson, with an efficiency assumed equal to one, while the other searches are inclusive. We also include in our analysis the dijet associated $\gamma\gamma$ production based on the full dataset [50, 51], with signal strengths and efficiencies² listed in Table II.

Within the class of models we will study, the part of the Lagrangian relevant for the

² We chose to include only the loose categories from the ATLAS and CMS dataset at 8 TeV.

	ATLAS 7TeV	ATLAS 8TeV	CMS 7TeV	CMS 8TeV
$\gamma\gamma JJ$	2.7 ± 1.9	2.8 ± 1.6	2.9 ± 1.9	0.3 ± 1.3
$pp \rightarrow h$	22.5%	45.0%	26.8%	46.8%
$pp \rightarrow qqh$	76.7%	54.1%	72.5%	51.1%
$pp \rightarrow t\bar{t}h$	0.6%	0.8%	0.6%	1.7%
$pp \rightarrow Vh$	0.1%	0.1%	0%	0.5%

TABLE II: Data on exclusive channels from LHC experiments.

recent LHC data is of the form

$$\begin{aligned}
\mathcal{L}_{\text{eff}} = & a_V \frac{2m_W^2}{v_w} h W_\mu^+ W^{-\mu} + a_V \frac{m_Z^2}{v_w} h Z_\mu Z^\mu - a_f \sum_{\psi=t,b,\tau} \frac{m_\psi}{v_w} h \bar{\psi} \psi \\
& + a_{V'} \frac{2m_{W'}^2}{v_w} h W_\mu'^+ W'^{-\mu} - a_S \frac{2m_S^2}{v_w} h S^+ S^-,
\end{aligned} \tag{2}$$

where the third and fourth terms involve, respectively, charged (but color singlet) vector and scalar bosons. We fix the mass parameters to the physical mass of the corresponding particle and v_w to the EW vacuum expectation value (vev), $v_w = 246$ GeV.

Consequently, the cross sections and branching rates relevant for Higgs physics are related to the corresponding quantities of the SM in a simple way. We define

$$\hat{\Gamma}_{ij} \equiv \frac{\Gamma_{h \rightarrow ij}}{\Gamma_{h_{\text{SM}} \rightarrow ij}^{\text{SM}}}, \quad \hat{\sigma}_\Omega \equiv \frac{\sigma_{\omega \rightarrow \Omega}}{\sigma_{\omega \rightarrow \Omega}^{\text{SM}}}, \tag{3}$$

and then, in terms of the coupling coefficients in Eq. (2), we have

$$\begin{aligned}
\hat{\sigma}_{hq} = \hat{\sigma}_{hA} = \hat{\Gamma}_{AA} = |a_V|^2, \quad \hat{\sigma}_{h\bar{t}t} = \hat{\sigma}_h = \hat{\Gamma}_{gg} = \hat{\Gamma}_{\psi\psi} = |a_f|^2, \\
A = W, Z \quad ; \quad \psi = b, \tau, c, \dots
\end{aligned} \tag{4}$$

where the gg and h final states are produced through a loop triangle diagram with only quarks as virtual particles.

The calculation of the Higgs decay rate to two photons is more involved. By using the formulas given in [52], we can write

$$\Gamma_{h \rightarrow \gamma\gamma} = \frac{\alpha_e^2 m_h^3}{256 \pi^3 v_w^2} \left| \sum_i N_i e_i^2 F_i \right|^2, \tag{5}$$

where the index i is summed over the SM charged particles as well as S^\pm and W'^\pm , N_i is the number of colors, e_i the electric charge in units of the electron charge, and the factors

F_i are defined by

$$\begin{aligned} F_A &= [2 + 3\tau_A + 3\tau_A(2 - \tau_A)f(\tau_A)]a_V, \quad A = W, W'; \\ F_\psi &= -2\tau_\psi[1 + (1 - \tau_\psi)f(\tau_\psi)]a_f, \quad \psi = t, b, \tau, \dots; \\ F_S &= \tau_S[1 - \tau_S f(\tau_S)]a_S, \quad \tau_i = \frac{4m_i^2}{m_h^2}, \end{aligned} \quad (6)$$

with

$$f(\tau_i) = \begin{cases} \arcsin^2 \sqrt{1/\tau_i} & \tau_i \geq 1 \\ -\frac{1}{4} \left[\log \frac{1 + \sqrt{1 - \tau_i}}{1 - \sqrt{1 - \tau_i}} - i\pi \right]^2 & \tau_i < 1 \end{cases}. \quad (7)$$

In the limit of heavy W'^\pm and S^\pm , one finds

$$F_{W'} = 7, \quad F_S = -\frac{1}{3}. \quad (8)$$

Given the experimental lower bounds on $m_{W'}$ and m_S [53, 54], the error on $F_{W'}$ is irrelevant while $|F_S|$ gets enhanced by about 10% for $m_S = 150$ GeV: since the experimental error on $\hat{\mu}_{\gamma\gamma}$ is large and constructive interference of the S^\pm and W^\pm is favored by the experiment, we also assume the error involved by the above approximation for F_S to be negligible.

We notice also that in the limit of heavy masses for the charged scalar and vector bosons the light Higgs decay to such (virtual) states is highly suppressed by kinematics, and therefore no additional decay channels have to be taken into account besides those of the SM.

To evaluate the theoretical predictions for the measured observables, we need the SM production cross sections for the Higgs boson and the SM branching ratios for its decay. The production cross sections at the LHC and Tevatron for the final state Ω are given [55] in Table III.

Ω	h	$q\bar{q}h$	$t\bar{t}h$	Wh	Zh	$h(X)$
7 TeV	15.31	1.211	0.08634	0.5729	0.3158	17.50
8 TeV	19.52	1.578	0.1302	0.6966	0.3943	22.32
1 TeV	0.9493	0.0653	0.0043	0.1295	0.0785	1.227

TABLE III: Standard Model Higgs production cross sections in units of pb.

The SM branching fractions are defined in terms of the decay rates, $\Gamma_{h \rightarrow ij}^{\text{SM}}$, as

$$\text{Br}_{ij}^{\text{SM}} = \frac{\Gamma_{h \rightarrow ij}^{\text{SM}}}{\Gamma_{\text{tot}}^{\text{SM}}}, \quad \Gamma_{\text{tot}}^{\text{SM}} = \sum_{ij=\bar{b}b, gg, WW, \dots} \Gamma_{h \rightarrow ij}^{\text{SM}} = 4.03 \text{ MeV}. \quad (9)$$

These are given [56] by

$$\text{Br}_{bb}^{\text{SM}} = 0.578, \quad \text{Br}_{\tau\bar{\tau}}^{\text{SM}} = 0.0637, \quad \text{Br}_{c\bar{c}}^{\text{SM}} = 0.0268, \quad \text{Br}_{gg}^{\text{SM}} = 0.0856, \quad (10)$$

$$\text{Br}_{\gamma\gamma}^{\text{SM}} = 0.0023, \quad \text{Br}_{\gamma Z}^{\text{SM}} = 0.00155, \quad \text{Br}_{WW}^{\text{SM}} = 0.216, \quad \text{Br}_{ZZ}^{\text{SM}} = 0.0267. \quad (11)$$

To determine the experimentally favored values of the free parameters $a_f, a_V, a_{V'}, a_S$, we minimize the quantity

$$\chi^2 = \sum_i \left(\frac{\mathcal{O}_i^{\text{exp}} - \mathcal{O}_i^{\text{th}}}{\sigma_i^{\text{exp}}} \right)^2, \quad (12)$$

where the measured values and errors of the observables are given in Tables I,II, while the numerical predictions of the theory are easily determined from Eqs. (3-8), with the SM input values given in Table III. In defining χ^2 above, we assumed the correlation matrix to be simply the identity matrix. We note that it is not possible to constrain both a_S and $a_{V'}$ since they both contribute only to the diphoton decay. The optimal values given below then refer to either of the two taken equal to zero:

$$a_V = 0.97_{-0.11}^{+0.10}, \quad a_f = 1.02_{-0.32}^{+0.25}, \quad \begin{cases} a_{V'} = 0.21_{-0.18}^{+0.16} \text{ and } a_S = 0 \\ a_{V'} = 0 \text{ and } a_S = -4.4_{-3.3}^{+3.8} \end{cases}, \quad (13)$$

with

$$\chi_{\min}^2/\text{d.o.f.} = 0.85, \quad P(\chi^2 > \chi_{\min}^2) = 62\%, \quad \text{d.o.f.} = 14. \quad (14)$$

The probability to get a minimum value of χ^2 larger than the optimal value above is naively expected to be around 50%, and therefore the corresponding value obtained above shows that the simple parametrization of Eq. (2) fits satisfactorily the data.

As a comparison, the SM produces

$$\chi_{\min}^2/\text{d.o.f.} = 0.92, \quad P(\chi^2 > \chi_{\min}^2) = 55\%, \quad \text{d.o.f.} = 17, \quad (15)$$

for only the Higgs physics data, which indeed is a rather ideal result. The inclusion of the EW parameters S and T ($S = T = 0$ for SM) [57–59] in the fit improves further the quality of the fit:

$$\chi_{\min}^2/\text{d.o.f.} = 0.89, \quad P(\chi^2 > \chi_{\min}^2) = 60\%, \quad \text{d.o.f.} = 19, \quad (16)$$

which shows that the SM is still perfectly viable in light of current collider data.

In the next section we use the Higgs physics constraints derived here to test the viability of a simple bosonic walking technicolor model [40] whose low energy effective Lagrangian belongs to the class specified by the generic Lagrangian of Eq. (2).

III. MODEL AND CONSTRAINTS

In Technicolor (TC) an additional, confining gauge interaction causes techniquarks, charged under TC and the EW interaction, to condense and break spontaneously the EW symmetry [31, 32]. This mechanism allows the W and Z bosons, and the composite states of the strongly coupled TC sector to acquire mass, while the SM fermions remain massless.

The TC sector we consider has $SU(2)_L \times SU(2)_R$ chiral symmetry and is described in terms of the complex composite meson field $M^T = (\phi^+, \phi^0)$ by an effective Lagrangian

$$\mathcal{L}_{\text{TC}} = D_\mu M^\dagger D^\mu M - m_M^2 M^\dagger M - \frac{\lambda_M}{3!} (M^\dagger M)^2. \quad (17)$$

To provide mass for ordinary matter fermions, an additional interaction linking them to the TC condensate has to be provided. In bosonic TC models, this link is provided by one (or more) elementary scalar(s) [60–64]. While in this paper we consider nonsupersymmetric theories, bosonic technicolor effective Lagrangians also arise as low energy realizations of supersymmetric technicolor theories [65–67]. In the context of bosonic TC, it is therefore the techniquark condensate that breaks EW symmetry, while the scalar plays the role of ”spectator”. The Higgs Lagrangian is written in terms of the usual complex doublet H as

$$\mathcal{L}_{\text{Higgs}} = D_\mu H^\dagger D^\mu H - m_H^2 H^\dagger H - \frac{\lambda_H}{3!} (H^\dagger H)^2. \quad (18)$$

The link between the technicolor and the SM matter fields obtained at the effective Lagrangian level is due to the Yukawa couplings of the Higgs field H . In addition to the usual couplings to the SM matter fields,

$$\mathcal{L}_{\text{Yuk}} = (y_u)_{ij} H \bar{Q}_i U_j + (y_d)_{ij} H^\dagger \bar{Q}_i D_j + (y_\ell)_{ij} H^\dagger \bar{L}_i E_j + \text{h.c.} , \quad (19)$$

these include also the couplings to techniquarks, $y_{TC} \bar{\Psi}_L H \Psi_R$. When constructing the effective Lagrangian for the composite sector of the theory, this coupling generates further terms in the effective TC Lagrangian so that the technicolor sector is described by [40]³

$$\begin{aligned} \mathcal{L}_{\text{bTC}} = & D_\mu M^\dagger D^\mu M - m_M^2 M^\dagger M - \frac{\lambda_M}{3!} (M^\dagger M)^2 \\ & + \left[c_3 y_{TC} D_\mu M^\dagger D^\mu H + c_1 y_{TC} f^2 M^\dagger H + \frac{c_2 y_{TC}}{3!} (M^\dagger M)(M^\dagger H) \right. \\ & \left. + \frac{c_4 y_{TC}}{3!} \lambda_H (H^\dagger H)(M^\dagger H) + \text{h.c.} \right] , \end{aligned} \quad (20)$$

³ Compared to the potential presented in [40], expressed in terms of matrix fields rather than EW doublets, we absorbed the ω factors in the c_i coefficients and pulled out a factor λ_H in front of c_4 , as suggested by naive dimensional analysis.

where c_i are unknown parameters and f is the vev of M . The model that we consider is therefore specified by the effective Lagrangian

$$\mathcal{L} = \mathcal{L}_{\text{SM}} + \mathcal{L}_{\text{bTC}}, \quad (21)$$

where \mathcal{L}_{SM} is the usual SM Lagrangian containing the sectors $\mathcal{L}_{\text{Higgs}}$ and \mathcal{L}_{Yuk} . The coefficients c_i in Eq. (20) are estimated by naive dimensional analysis [68, 69] to be

$$c_1 \sim \omega, \quad c_2 \sim \omega, \quad c_3 \sim \omega^{-1}, \quad c_4 \sim \omega^{-1}; \quad \omega \lesssim 4\pi. \quad (22)$$

Two of the parameters on the r.h.s. of Eqs. (18,20) are determined by the extremum conditions of the potential. Furthermore, the electroweak scale constrains the vevs of M and H by

$$v_w^2 = v^2 + f^2 + 2c_3 y_{TC} f v = (246 \text{ GeV})^2, \quad \langle M \rangle = \frac{f}{\sqrt{2}}, \quad \langle H \rangle = \frac{v}{\sqrt{2}}. \quad (23)$$

Finally, the requirement for the potential to be bounded from below imposes

$$\lambda_H, \lambda_M > 0; \quad \lambda_H + \lambda_M > 2(c_2 + c_4 \lambda_H) y_{TC}. \quad (24)$$

The mass eigenstates are obtained by diagonalizing first the kinetic terms and then applying a rotation to diagonalize the mass terms in the scalar and pseudoscalar sectors. First, the Higgs fields M and H are expressed as

$$\begin{pmatrix} M \\ H \end{pmatrix} = \frac{1}{\sqrt{2}} \begin{pmatrix} A & B \\ -A & B \end{pmatrix} \begin{pmatrix} M_2 \\ M_1 \end{pmatrix}, \quad A = (1 - c_3 y_{TC})^{-1/2}, \quad B = (1 + c_3 y_{TC})^{-1/2}. \quad (25)$$

After this transformation, the fields $M_{1,2}$ are written in terms of the charge eigenstates as

$$M_{1,2} = \begin{pmatrix} \Sigma_{1,2}^\pm \\ \frac{1}{\sqrt{2}}(f_{1,2} + \sigma_{1,2} + i\xi_{1,2}) \end{pmatrix}. \quad (26)$$

The rotation angles α and β determine the physical states in the scalar and pseudoscalar sectors so that the Goldstone bosons, G^\pm and G^0 , provide the respective longitudinal components of the W^\pm and Z bosons, while h^0, H^0, A^0 , and H^\pm are the neutral scalars, pseudoscalar, and charged scalar mass eigenstates, respectively:

$$\begin{pmatrix} h^0 \\ H^0 \end{pmatrix} = \begin{pmatrix} c_\alpha & -s_\alpha \\ s_\alpha & c_\alpha \end{pmatrix} \begin{pmatrix} \sigma_2 \\ \sigma_1 \end{pmatrix}, \quad \begin{pmatrix} G^0 \\ A^0 \end{pmatrix} = \begin{pmatrix} s_\beta & c_\beta \\ c_\beta & -s_\beta \end{pmatrix} \begin{pmatrix} \xi_2 \\ \xi_1 \end{pmatrix}, \quad \begin{pmatrix} G^\pm \\ H^\pm \end{pmatrix} = \begin{pmatrix} s_\beta & c_\beta \\ c_\beta & -s_\beta \end{pmatrix} \begin{pmatrix} \Sigma_2^\pm \\ \Sigma_1^\pm \end{pmatrix}. \quad (27)$$

The mixing angle β is defined so that $\tan \beta = f_2/f_1$. The masses of the lightest composite states, including neutral scalars, are naturally expected to be of $O(\Lambda_{TC}) \sim 1$ TeV. For bosonic TC the strong dynamics effect on the Higgs mass can be somewhat tamed by the mixing of the composite and elementary neutral scalar states, since the latter state can have a squared mass term much smaller than the former. This mechanism is analogous to the TeV-scale seesaw recently put forward in [70]. Moreover, it has been shown [71] that the top-quark loop contribution can greatly reduce the tree level TC prediction on the Higgs mass. A further suppression of the light Higgs mass is expected in NMWT because of walking dynamics [38]. From here on we assume that one or a combination of the mechanisms above is at work and use $m_{h^0} = 125 \pm 1$ GeV as an input to fix the value of one of the free parameters of the low energy effective theory.

To compare the model predictions with the LHC and Tevatron measurements, we need the coefficients of the SM Higgs linear couplings introduced in Eq. (2) to be expressed in terms of the bNMWT parameters:

$$\begin{aligned}
a_S = & \left[(c_{2\beta} - c_{2\rho}) \left((c_2 - c_4 \lambda_H) c_\rho^{-1} s_\rho^{-1} (c_{\alpha+3\beta} + c_{\alpha-\beta} c_{2\beta} c_{2\rho}) \right. \right. \\
& \left. \left. + 4 (c_2 + c_4 \lambda_H) c_\beta s_\beta (c_\alpha c_\beta t_\rho^{-2} + s_\alpha s_\beta t_\rho^2) \right) \right. \\
& \left. - (c_{\alpha-\rho} s_{2(\beta-\rho)}^2 s_{\beta+\rho} \lambda_H + c_{\alpha+\rho} s_{\beta-\rho} s_{2(\beta+\rho)}^2 \lambda_M) c_\rho^{-2} s_\rho^{-2} / y_{TC} \right] \\
& / \left[4 (c_4 \lambda_H s_{\beta-\rho}^2 + (12c_1 + c_2) s_{\beta+\rho}^2) \right] , \\
a_V = & s_{\beta-\alpha} , \quad a_f = \frac{c_{\alpha-\rho}}{s_{\beta-\rho}} ,
\end{aligned} \tag{28}$$

where $s_\alpha, c_\alpha, t_\alpha$ are shorthands for $\sin \alpha, \cos \alpha, \tan \alpha$, respectively, with α, β defined by the rotation matrices in Eq. (27) and ρ by

$$s_\rho = \sqrt{\frac{1 - c_3 y_{TC}}{2}} , \quad c_\rho = \sqrt{\frac{1 + c_3 y_{TC}}{2}} . \tag{29}$$

We are now ready to test the particle spectrum and its couplings against the latest experimental data. First, we scan the parameter space looking for data points that produce the right SM mass spectrum and satisfy the direct searches for charged particles at LEP [54] and a heavy neutral scalar at LHC [72] as well as the EW precision constraints from the S and T parameters [57–59]. More specifically, we impose the constraints

$$\begin{aligned}
m_{h^0} = & 125 \pm 1 \text{ GeV} , \quad m_{H^\pm} = m_{A^0} > 100 \text{ GeV} , \quad m_{H^0} > 600 \text{ GeV} , \quad \left| \frac{s_{\alpha-\rho}}{s_{\beta-\rho}} \right| < 1 , \\
S = & 0.04 \pm 0.09 , \quad T = 0.07 \pm 0.08 , \quad r(S, T) = 88\% , \quad m_{A^0}, m_{H^0} < 5\Lambda_{TC} .
\end{aligned} \tag{30}$$

The quantity $r(S, T)$ is the correlation coefficient for the S and T parameters [59]. The constraint on the trigonometric functions is to ensure that the heavy Higgs does not couple to SM fermions more strongly than a SM Higgs with the same mass does; this allows us to use straightforwardly the LHC constraint on m_{H^0} . The upper bounds on m_{A^0}, m_{H^0} are enforced by the cutoff of $O(\Lambda_{TC} \approx 4\pi v_w)$ of the effective Lagrangian. We also require the free parameters to produce the remaining SM mass spectrum and satisfy the bounds in Eq. (24). Then, we scan for such viable points in the domain

$$0 < \lambda_H, \lambda_M < (4\pi)^2, \quad 2\pi < |c_1|, |c_2|, |c_3^{-1}|, |c_4^{-1}| < 8\pi, \quad |c_3 y_{TC}| < 1 \\ |y_t| < 4\pi, \quad f = \pm \sqrt{v_w^2 - v^2 (1 - c_3^2 y_{TC}^2)} - v c_3 y_{TC}, \quad |v| < v_w (1 - c_3^2 y_{TC}^2)^{-1/2}, \quad (31)$$

with m_H^2, m_M^2 determined by the extremum conditions

$$\frac{\partial V}{\partial h^0} = 0, \quad \frac{\partial V}{\partial H^0} = 0, \quad (32)$$

where V is the scalar potential of the effective Lagrangian in Eqs. (18,20,21). The results that we present in the following of this section can be applied directly to the Type-I 2HDM by using the formulas in Appendix A. The disclaimer is that we are testing only a portion of the parameter space available to such a model, and more precisely the range of values typical for underlying strong dynamics.

The distribution of 5000 viable data points of the bNMWT allowed parameter space in the (S, T) plane is shown in Fig. 1. The 90% Confidence Level (CL) allowed region is shaded in green while the viable data points featuring $m_H^2 > 0$ ($m_H^2 < 0$) are plotted in black (grey). We make this distinction because for positive m_H^2 the SM Higgs sector alone would not break EW symmetry, and therefore EW symmetry breaking is generated through bosonic TC interactions. The black dots are, thus, relevant for bNMWT while the grey ones refer more generically to the Type-I 2HDM. It is clear that the viable region in S and T accessible by bNMWT is very limited.

In Fig. 2 we plot the viable data points in the (a_S, a_f) and (a_S, a_V) planes, respectively, together with the 68% (green), 90% (blue), and 95% (yellow) CL regions obtained in the previous section: these plots represent a slice of the a_f, a_V , and a_S parameter space passing through the optimal point (blue star) given in Eq. (13). There is a perfectly specular viable region, which we do not show here, intersecting another χ^2 global minimum point, obtained by flipping the signs of a_V, a_f , and a_S in Eq. (13). In Fig. 2, left panel, the upper viable

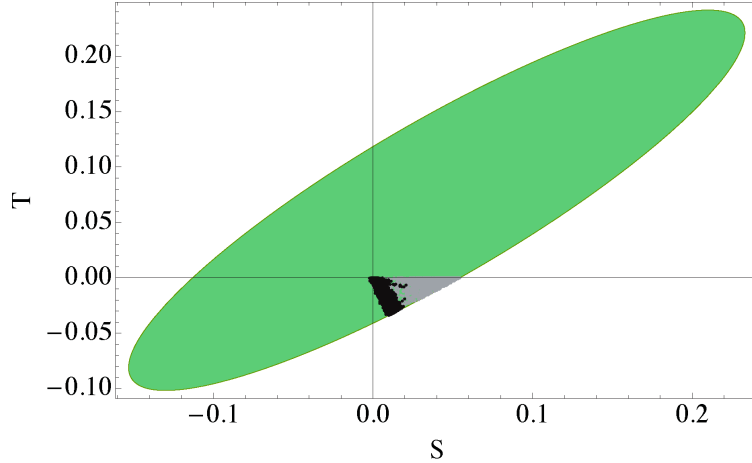


FIG. 1: 90%CL viable region (in green) of the precision EW parameters S and T : in black are the values relevant for bNMWT, while those in grey refer generically to Type-I 2HDM.

region, containing the best fit point, obtains the observed slight enhancement of the Higgs diphoton decay rate exclusively by the charged scalar contribution which interferes constructively with the W boson contribution. This results from a rather large linear coupling of h^0 to S^\pm . In the lower viable region, the slight enhancement of the Higgs diphoton decay rate is entirely due to the SM fermions which couple to h^0 with the same sign as W^\pm and, therefore, give constructive interference, while the scalar interferes destructively to balance an otherwise excessive enhancement of the decay rate to two photons. The same comments apply to the viable regions presented in Fig. 2, right panel.

The bNMWT data points are closely clustered around the SM values. This was somewhat expected, because of the small mixing of the two neutral Higgs fields for a heavy H mass. The choice of a heavy masses for the new states is naively dictated by strong dynamics, which in the scaled up QCD case would predict masses of $O(\Lambda_{TC}) \approx \text{TeV}$.

Finally, in Fig. 3 we show the bNMWT data points in the (a_V, a_f) plane that passes through the SM point ($a_S = a_f = a_V = 0$) to which they approximately belong. In bNMWT the Higgs-vector boson coupling is always reduced compared to its SM value, as shown in Fig. 3, while the experiment favors an enhancement of the same coupling. While bNMWT looks generally disfavored compared to the SM, most of the scanned data points lie within the 90% CL region.

We note that Fig. 1 also includes bNMWT points with flipped sign of a_f, a_V , and a_S . These points belong to the plane passing through the specular optimal point, and therefore

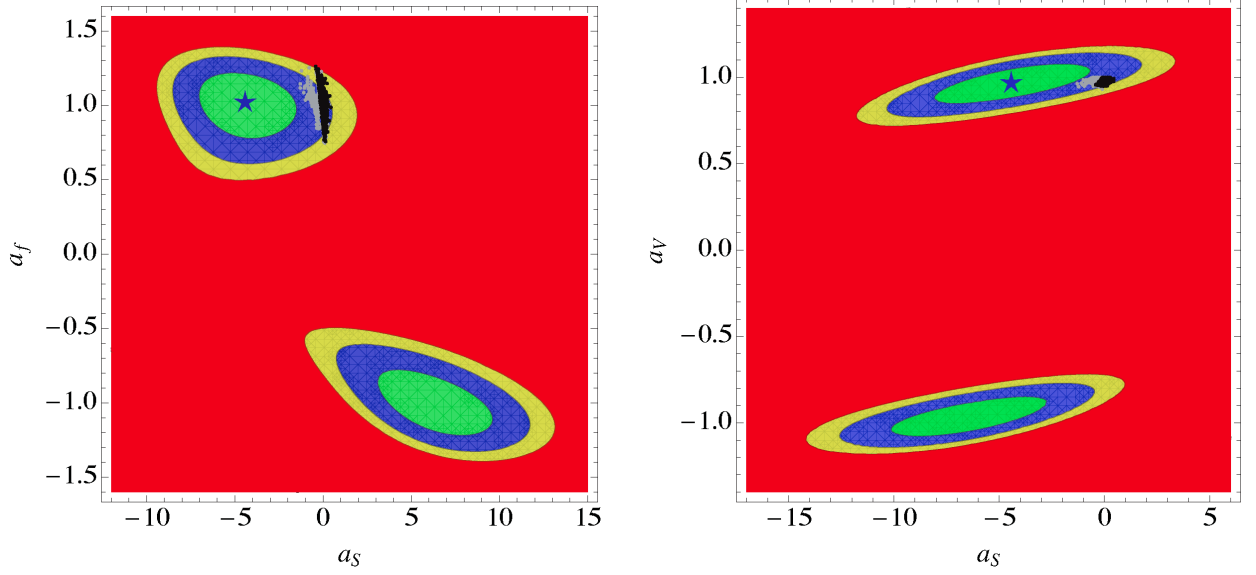


FIG. 2: Viable data points in the (a_S, a_f) (left pane) and (a_S, a_V) (right pane) planes, together with the 68% (green), 90% (blue), and 95% (yellow) CL region: in black are the values relevant for bNMWT while those in grey refer generically to Type-I 2HDM. The blue stars mark the optimal signal strengths on the respective planes intersecting the optimal point with $a_{V'} = 0$.

we do not include them in Figs. 2 and 3.

Among the scanned 5000 viable bNMWT data points featuring $m_H^2 > 0$, the one minimizing χ^2 is

$$a_V = 1.00, \quad a_f = 0.98, \quad a_S = 0.0, \quad S = T = 0 \quad \Rightarrow \quad \chi^2 = 16.73. \quad (33)$$

To estimate the goodness of fit of the scanned data points, we have to determine the number of degrees of freedom (d.o.f.) of the bNMWT parameter space, limited by the constraints motivated by strong dynamics. Since the free variables in the bNMWT Lagrangian in Eqs. (18,20) can be grouped in the coupling coefficients of Eq. (2), defined in terms of the TC Lagrangian variables by Eq. (28), one can expect the Higgs physics data presented in Section II to allow at most for three d.o.f., plus two since we also include the EW parameters S and T in the fit. In practice, the range of values found with the scan for a_S, a_V, S, T , is very small compared to the uncertainty affecting each of those parameters, and becomes negligible in the neighborhood of the best fit value of a_f due to a high correlation among all the five parameters. We assume, therefore, to have only one free parameter, a_f , which

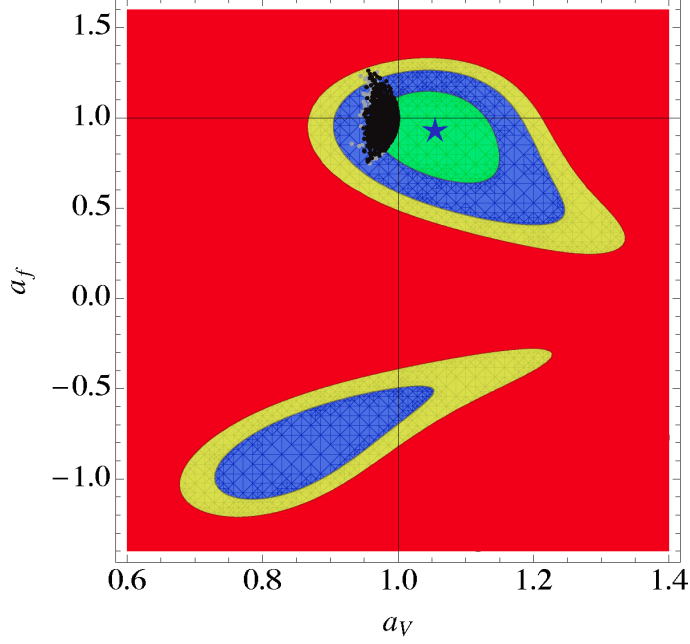


FIG. 3: Viable data points in the (a_V, a_f) plane, together with the 68% (green), 90% (blue), and 95% (yellow) CL region: in black are the values relevant for bNMWT while those in grey refer generically to Type-I 2HDM. The blue star marks the optimal signal strengths on the (a_V, a_f) plane for $a_S = a_{V'} = 0$.

produces the following statistical results:

$$\chi^2_{\min}/\text{d.o.f.} = 0.93, \quad P(\chi^2 > \chi^2_{\min}) = 54\%, \quad \text{d.o.f.} = 18. \quad (34)$$

These numbers should be compared to the corresponding results in the SM, Eq. (16), which indeed produces a better fit. Even without including S and T in the fit, we obtain the same optimal data point as the one in Eq. (33), with goodness of fit given by:

$$\chi^2_{\min}/\text{d.o.f.} = 0.97, \quad P(\chi^2 > \chi^2_{\min}) = 49\%, \quad \text{d.o.f.} = 16. \quad (35)$$

This result again is statistically worse than the relevant SM result, Eq. (15), and less appealing than the general fit result, Eq. (14).

For further comparison, we also give the corresponding results for the generic 2HDM data points ($m_H^2 < 0$):

$$\begin{aligned} a_V &= 0.99, \quad a_f = 0.93, \quad a_S = -1.2; \\ \chi^2_{\min}/\text{d.o.f.} &= 0.87, \quad P(\chi^2 > \chi^2_{\min}) = 60\%, \quad \text{d.o.f.} = 16. \end{aligned} \quad (36)$$

After adding the S and T parameters as well to the fit, we obtain

$$a_V = 1.00, \quad a_f = 0.99, \quad a_S = -0.4, \quad S = 0.01, \quad T = 0; \\ \chi_{\min}^2/\text{d.o.f.} = 0.91, \quad P(\chi^2 > \chi_{\min}^2) = 57\%, \quad \text{d.o.f.} = 18. \quad (37)$$

Indeed, the data points featuring $m_H^2 < 0$ produce a better fit than that of the bNMWT with EW symmetry breaking determined by strong dynamics, Eq. (34).

However, the results obtained so far for bNMWT do not take into account the contributions to Higgs physics coming from heavy charged vector bosons, which are a staple of strong dynamics. In the next section we study this subject by introducing some simple interaction terms in the Lagrangian and by working out the corresponding Higgs physics phenomenology.

IV. EXTRA CHARGED VECTOR BOSONS AND EXPERIMENTAL DATA FIT

Extra vector bosons arise naturally in TC as composite resonances with a mass of the order of the strong interaction scale Λ_{TC} . Of particular interest to us here is the possibility that an extra charged vector boson, W' , be responsible for the observed slight enhancement to the diphoton decay rate of the Higgs even if $m_{W'} \gg m_{h^0}$. Given the LHC constraints on the mass $m_{W'}$, equal to 2.55 TeV [53], it is safe to take the heavy W' limit, Eq. (8), for the Higgs decay rate to $\gamma\gamma$ in Eq. (5).

To introduce, in the effective Lagrangian, direct Higgs couplings to an extra massive vector boson which conserves gauge symmetry at the fundamental scale, we use the hidden local symmetry principle [73, 74], which has been already applied to NMWT in [39, 75]: here we just outline the main steps required to introduce composite vector bosons while conserving gauge invariance in the fundamental theory.

We begin by defining the following covariant derivatives

$$D^\mu N_L = \partial^\mu N_L + ig_L \tilde{W}^\mu N_L + ig_{TC} A_L^\mu N_L, \quad D^\mu N_R = \partial^\mu N_R + ig_Y \tilde{B}^\mu N_R + ig_{TC} A_R^\mu N_R, \quad (38)$$

where A_μ is the vector boson associated with the $G \equiv SU(2) \times SU(2)$ global symmetry of \mathcal{L}_{TC} , which we have gauged above, and N_L (N_R) is a scalar field in the fundamental of $SU(2)_L$ ($U(1)_Y$) and antifundamental of G . From the equations above, we can define a new

vector field and its transformation under the full gauged symmetry by

$$\text{Tr} \left[N_L N_L^\dagger \right] P_L^\mu = \frac{D^\mu N_L N_L^\dagger - N_L D^\mu N_L^\dagger}{ig_{TC}} , \quad P_L^\mu \rightarrow u_L P_L^\mu u_L^\dagger , \quad (39)$$

where u_L is a unitary transformation operator of $SU(2)$. The definition and transformation law of P_R are obtained simply by replacing L with R in Eq. (39). Among the possible dimension four, gauge invariant P^μ coupling terms to M , we retain only the following

$$\mathcal{L}_{M-P} = -g_{TC}^2 r_2 \text{Tr} [P_{L\mu} M' P_R^\mu M'^\dagger] + \frac{g_{TC}^2 r_1}{4} \text{Tr} [P_{L\mu}^2 + P_{R\mu}^2] \text{Tr} [M' M'^\dagger] , \quad (40)$$

where M' is the matrix representation of the EW doublet M . Assigning non-zero vevs for N_L and N_R , their kinetic terms generate a squared mass term for two vector boson combinations:

$$m_A^2 \text{Tr} [C_{L\mu}^2 + C_{R\mu}^2] , \quad C_L^\mu \equiv \langle P_L^\mu \rangle = A_L^\mu - \frac{g_L}{g_{TC}} \tilde{W}^\mu , \quad C_R^\mu \equiv \langle P_R^\mu \rangle = A_R^\mu - \frac{g_Y}{g_{TC}} \tilde{B}^\mu . \quad (41)$$

The resulting massless eigenstates give the ordinary W^μ and B^μ vector bosons, which instead acquire mass through EW symmetry breaking. In addition, there are two vector boson triplets, one vectorial (V^μ) and the other axial (A^μ). Since their interaction terms, given by Eq. (40) evaluated at the vev defined in Eq. (41), respect custodial symmetry and give the same contribution to the axial-axial and vector-vector EW vector boson polarization functions [76], the total contribution of the vector bosons to the EW precision parameters is identical to the SM one, and S and T are, therefore, zero [39, 75]. Moreover the vector boson contributions to FCNC have been tested against the experimental results and shown to be phenomenologically viable [77]. To simplify our analysis we fix

$$r_2 = -r_1 , \quad (42)$$

so that only \tilde{W}^μ and the vector resonance, V^μ , couple to the neutral Higgs fields.

The charged vector boson mass matrix in the (\tilde{W}, V, A) basis can be written in a compact form as

$$\begin{pmatrix} m_{\tilde{W}}^2 & -\frac{\epsilon m_V^2}{\sqrt{2}} & -\frac{\epsilon m_A^2}{\sqrt{2}} \\ -\frac{\epsilon m_V^2}{\sqrt{2}} & m_V^2 & 0 \\ -\frac{\epsilon m_A^2}{\sqrt{2}} & 0 & m_A^2 \end{pmatrix} , \quad (43)$$

with

$$m_{\tilde{W}}^2 = [x^2 + (1 + s^2) \epsilon^2] m_A^2 , \quad m_V^2 = (1 + 2s^2) m_A^2 , \quad (44)$$

and

$$s \equiv \frac{g_{TC} f}{2m_A} \sqrt{r_1} , \quad x \equiv \frac{g_L v_w}{2m_A} , \quad \epsilon \equiv \frac{g_L}{g_{TC}} . \quad (45)$$

We now study the implications of this setup in light of the LHC and Tevatron data fit we have at our disposal.

A. Mixing of Vector Fields

Let us begin with a rather general and simple case. We require that only \tilde{W} , the elementary gauge field, couples to h^0 , and therefore the W' coupling to the light Higgs is generated only through terms mixing \tilde{W} with the composite vector fields V and A . The squared mass matrix in the gauge basis (\tilde{W}, V, A) is obtained simply by setting $s = 0$ in Eqs. (43,44):

$$\begin{pmatrix} \frac{g_L^2 v_w^2}{4} + \epsilon^2 m_A^2 & -\frac{\epsilon m_A^2}{\sqrt{2}} & -\frac{\epsilon m_A^2}{\sqrt{2}} \\ -\frac{\epsilon m_A^2}{\sqrt{2}} & m_A^2 & 0 \\ -\frac{\epsilon m_A^2}{\sqrt{2}} & 0 & m_A^2 \end{pmatrix} . \quad (46)$$

We define the rotation to the mass eigenbasis in terms of x and ϵ , Eqs. (45), by

$$\begin{pmatrix} \tilde{W} \\ V \\ A \end{pmatrix} = \begin{pmatrix} c_\varphi & -s_\varphi & 0 \\ \frac{s_\varphi}{\sqrt{2}} & \frac{c_\varphi}{\sqrt{2}} & -\frac{1}{\sqrt{2}} \\ \frac{s_\varphi}{\sqrt{2}} & \frac{c_\varphi}{\sqrt{2}} & \frac{1}{\sqrt{2}} \end{pmatrix} \begin{pmatrix} W \\ W' \\ W'' \end{pmatrix} , \quad c_\varphi = \frac{1}{\sqrt{2}} \sqrt{1 + \frac{1 - x^2 - \epsilon^2}{\sqrt{(1 + x^2 + \epsilon^2)^2 - 4x^2}}} , \quad (47)$$

with corresponding eigenvalues

$$m_{W,W'}^2 = \frac{1}{2} \left[1 + x^2 + \epsilon^2 \mp \sqrt{(1 + x^2 + \epsilon^2)^2 - 4x^2} \right] m_A^2 , \quad m_{W''}^2 = m_A^2 . \quad (48)$$

The mixing matrix in Eq. (47) shows that only W and W' contribute to the gauge field \tilde{W} .

We checked that the Fermi coupling, G_F , determined by evaluating the amplitude for the muon decay ($\mu^- \rightarrow \nu_\mu \bar{\nu}_e e^-$), respects the usual relation

$$\sqrt{2} G_F = v_w^{-2} = (246 \text{ GeV})^{-2} . \quad (49)$$

The vector coupling coefficient a_V is suppressed, compared to the result in Eq. (28), because of mixing:

$$a_V = c_{\varphi'}^2 s_{\beta-\alpha} , \quad a_{V'} = s_{\varphi'}^2 s_{\beta-\alpha} , \quad (50)$$

with

$$c_{\varphi'}^2 = \frac{g_L^2 v_w^2}{4m_W^2} c_\varphi^2 = \frac{2x^2 \epsilon^2}{(1+x^2+\epsilon^2)^2 - 4x^2 - (1-x^2+\epsilon^2) \sqrt{(1+x^2+\epsilon^2)^2 - 4x^2}} . \quad (51)$$

The W'' coupling to h^0 is zero instead because we set $r_2 = -r_1$ in Eq. (40). Finally, the fermion and scalar coupling coefficients in Eq. (28) remain unchanged.

The lower limit on the mass of a sequential⁴ W' from direct searches at ATLAS [53], equal to 2.55 TeV at 95%CL, can be readily applied to the case above by properly rescaling the lower limit:

$$\Gamma_{W' \rightarrow l\nu} = \frac{g_{W'}^2 m_{W'}}{48\pi} \Rightarrow m_{W'} > (2.55 \text{ TeV}) \left(\frac{g_{W'}}{g_W} \right)^2, \quad \frac{g_{W'}}{g_W} = -s_{\varphi'} \frac{m_{W'}}{m_W}, \quad (52)$$

with $s_{\varphi'}$, $m_{W'}$, m_W defined in terms of x , ϵ , and m_A by Eqs. (51,48). By plotting the experimentally viable region defined by Eqs. (52) on the x and ϵ plane, we find the maximum allowed value of $\epsilon = 0.36$ (at the 95%CL), reached at $x = 0$ (equivalent to the limit of large m_A).

In strong dynamics the value of m_A is expected to be of $O(\text{TeV})$, which determines x to be of $O(10^{-2})$. In general this needs not to be the case, as larger values of x for small ϵ are allowed by the experiment. On the other hand we are interested primarily in testing bNMWT, and therefore in the following we will limit our analysis by assuming $x \ll 1$. This choice, moreover, guarantees that the W couplings do not change dramatically. Also, ϵ is expected to be small because of Eqs. (45) and the fact that $g_{TC} \gg g_L$. An expansion in both ϵ and x therefore produces

$$a_V = s_{\beta-\alpha} (1 - x^2 \epsilon^2) + O(x^n \epsilon^{5-n}), \quad a_{V'} = s_{\beta-\alpha} x^2 \epsilon^2 + O(x^n \epsilon^{5-n}), \quad n = 0, \dots, 5. \quad (53)$$

In this limit the effect of mixing on the W' and W couplings is negligible. Moreover, because the sum of a_V and $a_{V'}$ is independent of ϵ , so is the Higgs decay rate to two photons. Therefore, the optimal values for bNMWT with $m_A = 1 \text{ TeV}$, $\epsilon < 0.36$, and $m_H^2 > 0$ ($m_H^2 < 0$) correspond to the ones with no mixing ($\epsilon = 0$), presented in Eqs. (33) (Eqs. (37)).

In the next subsection we study the phenomenologically more appealing scenario in which the composite vector fields feature a direct coupling to neutral Higgs fields.

⁴ A sequential W' has the same couplings as the SM W .

B. Direct Higgs Coupling to W' and W''

Next we want to study the effects of a direct Higgs coupling to the composite vector field V , and consider $s \neq 0$. In this case, the charged vector boson mass matrix in the (\tilde{W}, V, A) basis is given by Eq. (43). The mass eigenvalues are lengthy cubic roots. These can be expanded in x and ϵ , which in TC are both expected to be small:

$$\begin{aligned} m_W^2 &\cong m_A^2 x^2 [1 - \epsilon^2] , & m_{W''}^2 &\cong m_A^2 \left[1 + \frac{1}{2} (1 + x^2) \epsilon^2 - \frac{1}{8} \left(2 + \frac{1}{s^2} \right) \epsilon^4 \right] , \\ m_{W'}^2 &\cong m_A^2 \left[1 + 2s^2 + \frac{1}{2} (1 + 2s^2 + x^2) \epsilon^2 + \frac{1}{8} \left(2 + \frac{1}{s^2} \right) \epsilon^4 \right] , \end{aligned} \quad (54)$$

where contributions of $O(x^n \epsilon^{5-n})$ are neglected, with $n = 0, \dots, 5$. The \tilde{W} and V coupling terms to the light Higgs can be derived from the mass matrix by taking its derivative with respect to v_w and introducing a factor ζ to take into account the rotation of M to the mass eigenbasis:

$$\mathcal{L} \subset \frac{2m_A^2}{v_w} s_{\beta-\alpha} \left[(x^2 + \zeta s^2 \epsilon^2) \tilde{W} \tilde{W} + 2\zeta s^2 V V - 2\sqrt{2} \zeta s^2 \epsilon \tilde{W} V \right] h^0 , \quad \zeta = s_{\beta-\alpha}^{-1} \frac{c_{\alpha+\rho}}{s_{\beta+\rho}} . \quad (55)$$

The vector boson coupling coefficients get an enhancement factor because of the s coupling:

$$a_V = \eta_W s_{\beta-\alpha} , \quad a_{V'} = (\eta_{W'} + \eta_{W''}) s_{\beta-\alpha} , \quad (56)$$

where

$$\begin{aligned} \eta_W &\cong 1 - \frac{[1 + s^2(3 - \zeta) + 2s^4] x^2 \epsilon^2}{(1 + 2s^2)^2} , & \eta_{W'} &\cong \frac{2\zeta s^2}{1 + 2s^2} + \frac{[1 + 2s^2(1 - \zeta)] x^2 \epsilon^2}{2(1 + 2s^2)^2} - \frac{\zeta \epsilon^4}{8s^2} , \\ \eta_{W''} &\cong \frac{x^2 \epsilon^2}{2} + \frac{\zeta \epsilon^4}{8s^2} , \end{aligned} \quad (57)$$

at $O(x^n \epsilon^{5-n})$, with $n = 0, \dots, 5$. We collected together the W' and W'' contributions to the Higgs decay to diphoton by summing up their respective coupling coefficients in Eq. (56).

It is interesting to notice that, at all orders in x :

$$\eta_W + \eta_{W'} + \eta_{W''} = 1 + \frac{2\zeta s^2}{1 + 2s^2} + O(\epsilon^5) . \quad (58)$$

The fermion and scalar coefficients are still determined by Eqs. (28). We obtain the optimal value of s by performing the global fit in the limit of negligible vector mixing ($\epsilon = 0$) and decoupled neutral heavy Higgs:

$$a_f = a_V = 1 , \quad a_S = 0 , \quad a_{V'} = \frac{2s^2}{1 + 2s^2} , \quad \Rightarrow \quad s = 0.32_{-0.32}^{+0.17} . \quad (59)$$

We use the same set of 5000 viable points scanned over the bNMWT parameter space with no W' and W'' , and re-calculate the coupling coefficients a_V and $a_{V'}$ at each data point for random values of s and ϵ , with $0 \leq s \leq 1$ and $0 \leq \epsilon \leq 0.1$, and $m_A = 1$ TeV. We plot the resulting bNMWT data points together with the experimentally favored regions in the $(a_V, a_{V'})$ and (a_V, a_f) planes in Fig. 4, and in the $(a_{V'}, a_f)$ plane in Fig 5, respectively, all passing through the optimal data point defined in Eq. (13). The plots are again limited to the positive a_V half-plane. For $m_H^2 < 0$ the mixing factor ζ , Eq. (55), can be negative, which makes $a_{V'}$ flip sign, compared to a_V , because of Eqs. (57). Already by visual inspection, it

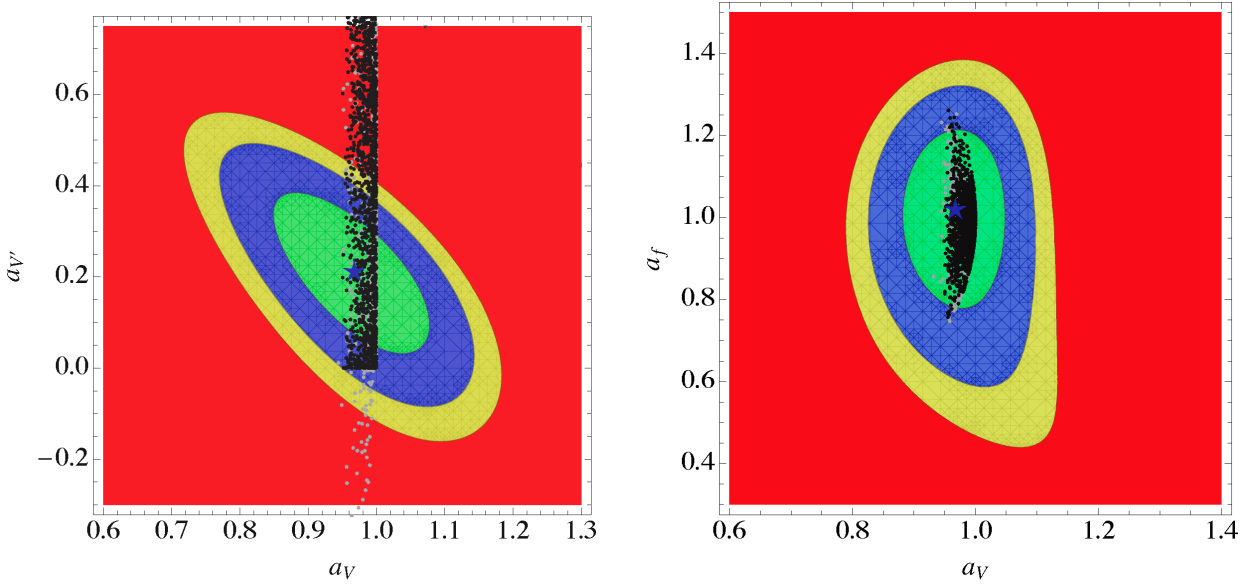


FIG. 4: Viable data points in the $(a_V, a_{V'})$ and (a_V, a_f) planes, together with the 68% (green), 90% (blue), and 95% (yellow) CL region: in black are the values relevant for bNMWT while those in grey refer generically to Type-I 2HDM with the addition of two charged vector bosons. The blue stars mark the optimal signal strengths on the respective planes intersecting the optimal point with $a_S = 0$.

is clear that the s coupling allows bNMWT to cover a large portion of the 68% CL favored region. We verified that all the three parameters a_f , $a_{V'}$, and (to a lesser degree) a_V are free (meaning that they are little correlated and with a range of values comparable to the error affecting the optimal values in Eq. (13)), which was expected since we introduced two new

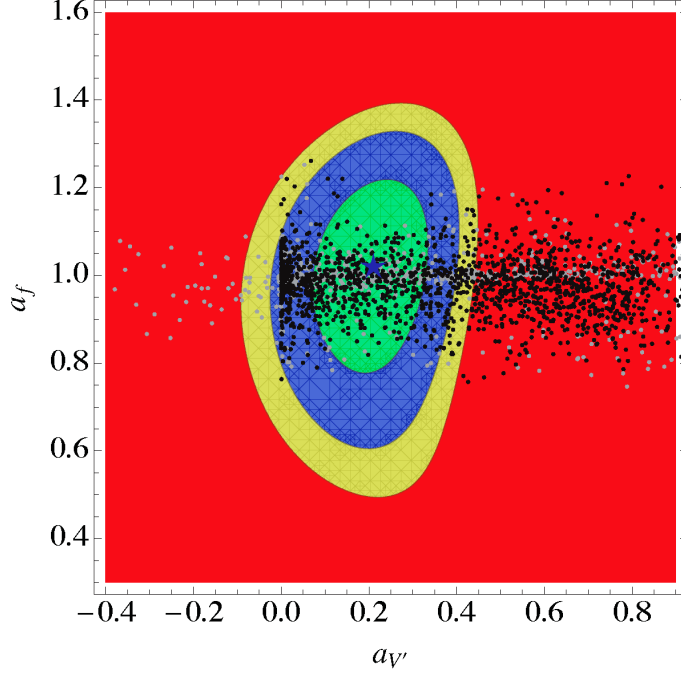


FIG. 5: Viable data points in the $(a_{V'}, a_f)$ plane, together with the 68% (green), 90% (blue), and 95% (yellow) CL region: in black are the values relevant for bNMWT while those in grey refer generically to Type-I 2HDM with the addition of two charged vector bosons. The blue star marks the optimal signal strengths on the $(a_{V'}, a_f)$ plane for optimal a_V and with $a_S = 0$.

parameters, ϵ and s . In this case the bNMWT data point minimizing χ^2 for $m_H^2 > 0$ is

$$\begin{aligned} a_V &= 1.00, & a_f &= 1.00, & a_{V'} &= 0.19, & a_S &= 0.0, & S &= T = 0.00; \\ \chi_{\min}^2/\text{d.o.f.} &= 0.83, & P(\chi^2 > \chi_{\min}^2) &= 65\%, & \text{d.o.f.} &= 16, \end{aligned} \quad (60)$$

while for $m_H^2 < 0$ we find

$$\begin{aligned} a_V &= 1.00, & a_f &= 0.98, & a_{V'} &= 0.18, & a_S &= 0.0, & S &= T = 0.00; \\ \chi_{\min}^2/\text{d.o.f.} &= 0.83, & P(\chi^2 > \chi_{\min}^2) &= 65\%, & \text{d.o.f.} &= 16. \end{aligned} \quad (61)$$

The cases above are equally favored by the experiment and both feature a probability greater than the one for the general fit, Eq. (13), which does not include the S and T EW parameters (and therefore has two less d.o.f.) but gives a similar value of χ_{\min}^2 . As a last remark, we note that $a_{V'}$ is rather unconstrained by the chosen set of observables, and so a broader set of observables related to W' physics would be necessary to further test the viability of bNMWT.

V. CONCLUSIONS AND OUTLOOK

In this paper we have considered quantitatively how much the coefficients of Higgs couplings to electroweak gauge bosons (a_V) and fermions (a_f) as well as to possible extra scalars (a_S) can deviate from their corresponding values in the Standard Model ($a_V = a_f = 1$, $a_S = 0$) in light of the current LHC and Tevatron data. We then considered a bosonic technicolor model, bNMWT [40], and studied its viability by performing a scan on the parameter space which implements the direct constraints on the mass spectrum as well as the constraints from precision EW data (in terms of the S and T parameters). The scalar sector of the bosonic technicolor model we considered can be more generally viewed as a type-I 2HDM.

The essential consequence of underlying strong dynamics is the existence of new vector resonances in the particle spectrum. We implemented these new states in an effective Lagrangian to study their effects. We considered in detail the implications of the effective Lagrangian on the couplings of the Higgs boson to the physical W and Z bosons as well as to fermions. Then, we studied first the simple case of minimal coupling to the SM fields, which amounts to considering only the mixing of the two new triplets of vector bosons and the $SU(2)_L$ gauge fields without direct interaction between the composite vector bosons and SM fields. In this simple scenario we determined the 95%CL upper bound on the amount of mixing allowed by experimental data. We showed that this generic scenario in bNMWT cannot be resolved by the current data.

Finally we illustrated the possible effects of the direct coupling between composite vector bosons and neutral scalar fields within our effective Lagrangian scheme. We showed that the direct coupling allows for an optimal fit by the bNMWT predictions of the current experimental data. A more refined analysis of the model including additional observables can further test the possibility of a strongly coupled sector underlying the electroweak sector of the SM.

Acknowledgments

The support from Finnish Cultural Foundation, Central Finland Regional fund is gratefully acknowledged.

Appendix A: Two Higgs Doublet Model Potential

Let us write our bosonic technicolor Lagrangian explicitly as a two-Higgs doublet model (2HDM). The starting point is given by Eqs.(20,21). The kinetic mixing term in Eq.(20) is rotated away and the model canonically normalized by Eq.(25). Applying one more rotation we can express the SM Yukawa couplings in the following form

$$\mathcal{L}_{\text{Yuk}} = (y_u)_{ij} K H_2 \bar{Q}_i U_j + (y_d)_{ij} K H_2^\dagger \bar{Q}_i D_j + (y_\ell)_{ij} K H_2^\dagger \bar{L}_i E_j + \text{h.c.} , \quad K = (1 - c_3^2 y_{TC}^2)^{-\frac{1}{2}} , \quad (\text{A1})$$

where the full transformation is given by

$$H = K H_2 , \quad M = H_1 - c_3 y_{TC} K H_2 . \quad (\text{A2})$$

As Eq. (A1) shows, only one of the two Higgses (by convention H_2) couples to SM fermions, which ensures that there are no tree-level contributions to Flavor Changing Neutral Currents (FCNC): such a model in literature has been referred to as Type-I 2HDM [41].

On the other hand, the most general renormalizable Higgs potential of a 2HDM can be written as

$$\begin{aligned} V = & m_1^2 H_1^\dagger H_1 + m_2^2 H_2^\dagger H_2 - m_{12}^2 (H_1^\dagger H_2 + H_2^\dagger H_1) + \frac{\lambda_1}{2} (H_1^\dagger H_1)^2 + \frac{\lambda_2}{2} (H_2^\dagger H_2)^2 \\ & + \lambda_3 (H_1^\dagger H_1)(H_2^\dagger H_2) + \lambda_4 (H_2^\dagger H_1)(H_1^\dagger H_2) + \left[\frac{\lambda_5}{2} (H_1^\dagger H_2)^2 \right. \\ & \left. - \lambda_6 (H_2^\dagger H_1)(H_1^\dagger H_1) - \lambda_7 (H_2^\dagger H_1)(H_2^\dagger H_2) + \text{h.c.} \right] . \end{aligned} \quad (\text{A3})$$

The coefficients in Eq. (A3) can be expressed in terms of those in the potential $V(M, H)$, in the notation of [40], by:

$$\begin{aligned} m_1^2 &= m_M^2 , \quad m_2^2 = [m_H^2 + (2f^2 c_1 + m_M^2 c_3) c_3 y_{TC}^2] K^2 , \quad m_{12}^2 = (f^2 c_1 + m_M^2 c_3) y_{TC} K , \\ \lambda_1 &= \frac{1}{3} \lambda_M , \quad \lambda_2 = \frac{1}{3} (2c_2 c_3^3 y_{TC}^4 + \lambda_H + 2c_3 c_4 y_{TC}^2 \lambda_H + c_3^4 y_{TC}^4 \lambda_M) K^4 , \\ \lambda_3 &= \lambda_4 = \lambda_5 = \frac{1}{6} (c_2 + c_3 \lambda_M) c_3 y_{TC}^2 K^2 , \\ \lambda_6 &= \frac{1}{6} (c_2 + 2c_3 \lambda_M) y_{TC} K , \quad \lambda_7 = \frac{1}{6} [c_4 \lambda_H + c_3^2 y_{TC}^2 (3c_2 + 2c_3 \lambda_M)] y_{TC} K^3 , \end{aligned} \quad (\text{A4})$$

The Higgs fields in Eq. (A3) are expressed in terms of the real degrees of freedom by

$$H_i = \begin{pmatrix} H_i^+ \\ \frac{1}{\sqrt{2}}(v_i + h_i + i\phi_i) \end{pmatrix} , \quad i = 1, 2 ; \tan \beta' \equiv \frac{v_1}{v_2} . \quad (\text{A5})$$

The Goldstone boson G^\pm (G^0) provides the longitudinal components of the W^\pm (Z^0) boson, while h^0 , H^0 , A^0 , and H^\pm are the neutral scalars, pseudoscalar, and charged scalar mass eigenstates, respectively:

$$\begin{aligned} \begin{pmatrix} h^0 \\ H^0 \end{pmatrix} &= \begin{pmatrix} c_{\alpha'} & -s_{\alpha'} \\ s_{\alpha'} & c_{\alpha'} \end{pmatrix} \begin{pmatrix} h_1 \\ h_2 \end{pmatrix}, \quad \begin{pmatrix} G^0 \\ A^0 \end{pmatrix} = \begin{pmatrix} s_{\beta'} & c_{\beta'} \\ c_{\beta'} & -s_{\beta'} \end{pmatrix} \begin{pmatrix} \phi_1 \\ \phi_2 \end{pmatrix}, \\ \begin{pmatrix} G^\pm \\ H^\pm \end{pmatrix} &= \begin{pmatrix} s_{\beta'} & c_{\beta'} \\ c_{\beta'} & -s_{\beta'} \end{pmatrix} \begin{pmatrix} H_1^\pm \\ H_2^\pm \end{pmatrix}. \end{aligned} \quad (\text{A6})$$

The angles α', β' differ from α, β only because of the extra rotation in Eq.(A2) that makes only H_2 couple to SM fermions.

-
- [1] A. Azatov, R. Contino and J. Galloway, JHEP **1204**, 127 (2012) [arXiv:1202.3415 [hep-ph]].
 - [2] D. Carmi, A. Falkowski, E. Kuflik and T. Volansky, JHEP **1207**, 136 (2012) [arXiv:1202.3144 [hep-ph]].
 - [3] J. R. Espinosa, C. Grojean, M. Muhlleitner and M. Trott, JHEP **1205**, 097 (2012) [arXiv:1202.3697 [hep-ph]].
 - [4] P. P. Giardino, K. Kannike, M. Raidal and A. Strumia, JHEP **1206**, 117 (2012) [arXiv:1203.4254 [hep-ph]].
 - [5] M. Carena, I. Low and C. E. M. Wagner, JHEP **1208**, 060 (2012) [arXiv:1206.1082 [hep-ph]].
 - [6] T. Corbett, O. J. P. Eboli, J. Gonzalez-Fraile, M. C. Gonzalez-Garcia and , Phys. Rev. D **86**, 075013 (2012) [arXiv:1207.1344 [hep-ph]].
 - [7] P. P. Giardino, K. Kannike, M. Raidal and A. Strumia, Phys. Lett. B **718**, 469 (2012) [arXiv:1207.1347 [hep-ph]].
 - [8] J. Ellis and T. You, JHEP **1209**, 123 (2012) [arXiv:1207.1693 [hep-ph]].
 - [9] D. Carmi, A. Falkowski, E. Kuflik, T. Volansky and J. Zupan, JHEP **1210**, 196 (2012) [arXiv:1207.1718 [hep-ph]].
 - [10] S. Banerjee, S. Mukhopadhyay, B. Mukhopadhyaya and , JHEP **1210** (2012) 062 [arXiv:1207.3588 [hep-ph]].
 - [11] N. Arkani-Hamed, K. Blum, R. T. D'Agnolo and J. Fan, JHEP **1301**, 149 (2013) [arXiv:1207.4482 [hep-ph]].

- [12] F. Bonnet, T. Ota, M. Rauch, W. Winter and , Phys. Rev. D **86**, 093014 (2012) [arXiv:1207.4599 [hep-ph]].
- [13] T. Corbett, O. J. P. Eboli, J. Gonzalez-Fraile, M. C. Gonzalez-Garcia and , Phys. Rev. D **87**, 015022 (2013) [arXiv:1211.4580 [hep-ph]].
- [14] ATLAS collaboration, conference note ATLAS-CONF-2013-012
- [15] CMS collaboration, note CMS-PAS-HIG-13-001
- [16] C. a. D. Group [Tevatron New Physics Higgs Working Group and CDF Collaboration and D0], Moriond EW 2013 update, arXiv:1207.0449 [hep-ex].
- [17] M. Carena, S. Gori, N. R. Shah, C. E. M. Wagner and L. T. M. Wang, JHEP **1207**, 175 (2012) [arXiv:1205.5842 [hep-ph]].
- [18] A. Arbey, M. Battaglia, A. Djouadi and F. Mahmoudi, JHEP **1209**, 107 (2012) [arXiv:1207.1348 [hep-ph]].
- [19] J. J. Cao, Z. X. Heng, J. M. Yang, Y. M. Zhang and J. Y. Zhu, JHEP **1203**, 086 (2012) [arXiv:1202.5821 [hep-ph]].
- [20] N. D. Christensen, T. Han and S. Su, Phys. Rev. D **85**, 115018 (2012) [arXiv:1203.3207 [hep-ph]].
- [21] J. F. Gunion, Y. Jiang and S. Kraml, Phys. Lett. B **710**, 454 (2012) [arXiv:1201.0982 [hep-ph]].
- [22] S. F. King, M. Muhlleitner and R. Nevzorov, Nucl. Phys. B **860**, 207 (2012) [arXiv:1201.2671 [hep-ph]].
- [23] J. Ellis and K. A. Olive, Eur. Phys. J. C **72**, 2005 (2012) [arXiv:1202.3262 [hep-ph]].
- [24] R. Contino, D. Marzocca, D. Pappadopulo and R. Rattazzi, JHEP **1110**, 081 (2011) [arXiv:1109.1570 [hep-ph]].
- [25] J. R. Espinosa, C. Grojean and M. Muhlleitner, EPJ Web Conf. **28**, 08004 (2012) [arXiv:1202.1286 [hep-ph]].
- [26] N. Haba, K. Kaneta, Y. Mimura and R. Takahashi, Phys. Lett. B **718**, 1441 (2013) [arXiv:1207.5102 [hep-ph]].
- [27] M. T. Frandsen and F. Sannino, arXiv:1203.3988 [hep-ph].
- [28] C. Du, H. -J. He, Y. -P. Kuang, B. Zhang, N. D. Christensen, R. S. Chivukula and E. H. Simmons, Phys. Rev. D **86**, 095011 (2012) [arXiv:1206.6022 [hep-ph]].
- [29] T. Abe, N. Chen and H. -J. He, JHEP **1301**, 082 (2013) [arXiv:1207.4103 [hep-ph]].
- [30] J. R. Andersen, T. Hapola, F. Sannino and , Phys. Rev. D **85**, 055017 (2012) [arXiv:1105.1433

- [hep-ph]].
- [31] S. Dimopoulos and L. Susskind, Nucl. Phys. B **155**, 237 (1979).
 - [32] E. Farhi and L. Susskind, Phys. Rept. **74**, 277 (1981).
 - [33] N. Arkani-Hamed, A. G. Cohen, E. Katz and A. E. Nelson, JHEP **0207**, 034 (2002) [arXiv:hep-ph/0206021].
 - [34] N. Arkani-Hamed, A. G. Cohen, E. Katz, A. E. Nelson, T. Gregoire and J. G. Wacker, JHEP **0208**, 021 (2002) [arXiv:hep-ph/0206020].
 - [35] L. Randall and R. Sundrum, Phys. Rev. Lett. **83**, 3370 (1999) [arXiv:hep-ph/9905221].
 - [36] N. Arkani-Hamed, S. Dimopoulos and G. R. Dvali, Phys. Lett. B **429**, 263 (1998) [arXiv:hep-ph/9803315].
 - [37] F. Sannino and K. Tuominen, Phys. Rev. D **71**, 051901 (2005) [arXiv:hep-ph/0405209].
 - [38] D. D. Dietrich, F. Sannino and K. Tuominen, Phys. Rev. D **72**, 055001 (2005) [arXiv:hep-ph/0505059].
 - [39] A. Belyaev, R. Foadi, M. T. Frandsen, M. Jarvinen, F. Sannino and A. Pukhov, Phys. Rev. D **79**, 035006 (2009) [arXiv:0809.0793 [hep-ph]].
 - [40] M. Antola, M. Heikinheimo, F. Sannino and K. Tuominen, JHEP **1003**, 050 (2010) [arXiv:0910.3681 [hep-ph]].
 - [41] G. C. Branco, P. M. Ferreira, L. Lavoura, M. N. Rebelo, M. Sher and J. P. Silva, Phys. Rept. **516**, 1 (2012) [arXiv:1106.0034 [hep-ph]].
 - [42] ATLAS collaboration, conference note ATLAS-CONF-2013-030
 - [43] ATLAS collaboration, conference note ATLAS-CONF-2013-013
 - [44] CMS collaboration, conference note CMS-PAS-HIG-13-003
 - [45] CMS collaboration, conference note CMS-PAS-HIG-13-002
 - [46] CMS collaboration, conference note CMS-PAS-HIG-13-004
 - [47] ATLAS collaboration, conference note ATLAS-CONF-2012-161
 - [48] CMS collaboration, conference note CMS-PAS-HIG-12-044
 - [49] ATLAS collaboration, conference note ATLAS-CONF-2012-160
 - [50] ATLAS collaboration, conference notes ATLAS-CONF-2012-091, ATLAS-CONF-2013-012
 - [51] CMS collaboration, conference note CMS-PAS-HIG-13-001
 - [52] J. F. Gunion, H. E. Haber, G. L. Kane and S. Dawson, Front. Phys. **80**, 1 (2000).
 - [53] ATLAS collaboration, conference note ATLAS-CONF-2012-086

- [54] A. Heister *et al.* [ALEPH Collaboration], Phys. Lett. B **543**, 1 (2002) [arXiv:hep-ex/0207054].
- [55] S. Dittmaier *et al.* [LHC Higgs Cross Section Working Group], arXiv:1101.0593 [hep-ph].
- [56] S. Dittmaier *et al.*, arXiv:1201.3084 [hep-ph].
- [57] M. E. Peskin and T. Takeuchi, Phys. Rev. D **46**, 381 (1992).
- [58] H. J. He, N. Polonsky and S. f. Su, Phys. Rev. D **64**, 053004 (2001) [arXiv:hep-ph/0102144].
- [59] J. Beringer et al. (Particle Data Group), Phys. Rev. D **86**, 010001 (2012)
- [60] E. H. Simmons, Nucl. Phys. B **312**, 253 (1989).
- [61] S. Samuel, Nucl. Phys. B **347**, 625 (1990).
- [62] A. Kagan and S. Samuel, Phys. Lett. B **270**, 37 (1991).
- [63] C. D. Carone and E. H. Simmons, Nucl. Phys. B **397**, 591 (1993) [arXiv:hep-ph/9207273].
- [64] V. Hemmige and E. H. Simmons, Phys. Lett. B **518**, 72 (2001) [arXiv:hep-ph/0107117].
- [65] M. Dine, W. Fischler and M. Srednicki, Nucl. Phys. B **189**, 575 (1981).
- [66] M. Antola, S. Di Chiara, F. Sannino and K. Tuominen, Eur. Phys. J. C **71**, 1784 (2011) [arXiv:1001.2040 [hep-ph]].
- [67] M. Antola, S. Di Chiara, F. Sannino, K. Tuominen, Nucl. Phys. B **864**, 664 (2012) [arXiv:1111.1009 [hep-ph]].
- [68] A. Manohar and H. Georgi, Nucl. Phys. B **234**, 189 (1984).
- [69] A. G. Cohen, D. B. Kaplan and A. E. Nelson, Phys. Lett. B **412**, 301 (1997) [arXiv:hep-ph/9706275].
- [70] R. Foadi and M. T. Frandsen, arXiv:1212.0015 [hep-ph].
- [71] R. Foadi, M. T. Frandsen and F. Sannino, arXiv:1211.1083 [hep-ph].
- [72] S. Chatrchyan [CMS Collaboration], Phys. Lett. B **710**, 26 (2012) [arXiv:1202.1488 [hep-ex]].
- [73] M. Bando, T. Kugo, S. Uehara, K. Yamawaki and T. Yanagida, Phys. Rev. Lett. **54**, 1215 (1985).
- [74] M. Bando, T. Kugo and K. Yamawaki, Phys. Rept. **164**, 217 (1988).
- [75] R. Foadi, M. T. Frandsen, T. A. Ryttov and F. Sannino, Phys. Rev. D **76**, 055005 (2007) [arXiv:0706.1696 [hep-ph]].
- [76] M. E. Peskin and T. Takeuchi, Phys. Rev. Lett. **65**, 964 (1990).
- [77] H. S. Fukano, M. Heikinheimo and K. Tuominen, Phys. Rev. D **84**, 035017 (2011) [arXiv:1106.2433 [hep-ph]].